

Received December 7, 2019, accepted December 18, 2019, date of publication December 23, 2019, date of current version December 31, 2019.

Digital Object Identifier 10.1109/ACCESS.2019.2961425

Design and Implementation of a Self-Starting Permanent Magnet Hysteresis Synchronous Motor for Pump Applications

MEHMET GEDİKPINAR 

Electrical and Electronics Engineering Department, Firat University, 23119 Elazig, Turkey

e-mail: mgedikpinar@firat.edu.tr

ABSTRACT A Permanent Magnet Hysteresis Synchronous Motor (PMHSM) is designed and implemented in this paper. The designed motor is analyzed by using simulation and experimental studies. The torque, torque ripple, speed and flux density are also analyzed by using Finite Element Analysis (FEA) method. A standard commercial stator geometry is preferred for easy installation. A new rotor structure is designed for the motor. A submersible pump turbine is connected to the prototype motor in order to test under a real pump load condition by a pump test stand. The same pump used in the experiment was also tested with a commercial induction motor (IM) submersible pump motor with same power. Thus, the commercial and proposed motor are compared in terms of static head value, which is an important value in pump applications. The performance of the motor is better than the IM because it can operate at synchronous speed without slip. In addition, the proposed motor does not require any auxiliary system to achieve starting with grid. The proposed PMHSM can be used to obtain high performance and efficiency for pump applications.


INDEX TERMS AC machine, hysteresis motor, permanent magnet motor, pump, hybrid rotor.

I. INTRODUCTION

The limited energy resources of the world are decreasing rapidly because energy consumption increases day by day. Therefore, efficient systems should be used to reduce energy consumption. Electric motors consume almost half of the electricity produced in the world [1]. Due to its many advantages, induction motors are widely used in industrial applications. However, these motors are known to have lower efficiency than synchronous motors [2]. The efficiency classes of induction motors are called IE1, IE2 and IE3. However, single-phase IMs have not high efficiency some studies on efficient motors have been presented in the literature [3]–[5]. Nowadays, Permanent Magnet Synchronous Motors (PMSM) and Brushless DC (BLDC) Motors have been started used in order to obtain high efficiency. This type of motors cannot directly connect to the grid and they require expensive drive systems to operate. This is a disadvantage, especially for low power applications. In addition, the motor drive circuits produce undesirable harmonics over the grid and reduce power quality. Whereas proposed hysteresis

synchronous motor does not require any auxiliary starting equipment as the other synchronous motors. Several studies in the literature have focused on the hybrid rotor structure to improve motor performance [6].

The performed motor in this study is a hybrid hysteresis motor type which can start directly by connecting from the grid without need a motor drive. The stator structure of the motor can be used same structure of a traditional three-phase IMs. However, the proposed rotor structure is completely different from that of traditional IM. This difference in the rotor structure improves the motor performance. Traditional IM motors are used the squirrel cage rotor. The squirrel cage is not easily manufactured in mass production. Generally, aluminum bars are used in the squirrel cages which are required casting and injection molding machine. These process needs time, labor cost and material cost. So we need to use an easy ring instead of the squirrel cage. Thus, the motor type changes from asynchronous to synchronous [7]–[12]. There are various studies on line-start permanent magnet synchronous motors without using hysteresis ring in the literature [12]–[14]. Rotor position measurement is not required for start-up and synchronization of this motor unlike other synchronous motors [15], [16]. Classic IMs are widely used

The associate editor coordinating the review of this manuscript and approving it for publication was Kan Liu .

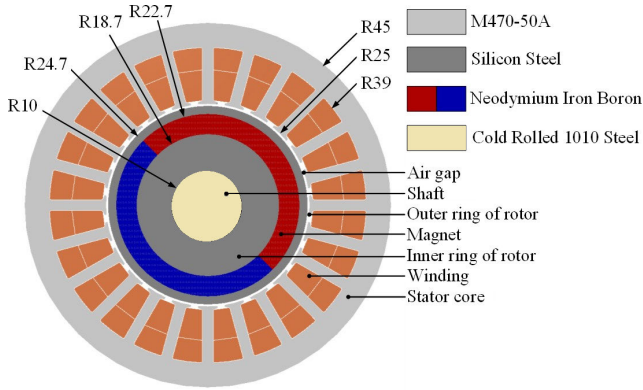


FIGURE 1. The structure of stator and rotor.

for submersible pumps, fire pumps, jet pumps, oil well pumps, and circulation pumps. IMs have rotor slip under load conditions when IMs are used as pump motor. The speed of pump fans is considerably reduced due to slip the efficiency of the pump system is reduced because there is an exponentially decreasing relationship between the load and the speed of the pump [17], [18]. The stator and rotor structure of the designed motor are given in Figure 1. As shown in the figure, the stator structure is same to the stator of a traditional IM. However, the proposed rotor structure is completely different from commercial rotor structures. The designed rotor structure consists of two hysteresis ring structures as called inner ring and outer ring and permanent magnets interposed between them. In this study, a novel rotor type that can start without any drive circuit is designed to allow connection to direct grid. The designed motor is analyzed by using simulation environment. The proposed motor is tested connected to a submersible pump. Same pump system is tested with an IM having the same power value to obtain a good comparison between proposed motor and commercial motor. The proposed motor is achieved satisfactory results such as high power/volume, slip-free steady-state operation, increased pumping performance, and ease of mass manufacture of the rotor when compared to the same powered IM. Synchronous speed operation of the motor is very important in order to increase the efficiency of the submersible pump system. For this reason, it is aimed to use synchronous motor which can start with directly connected to grid in order to solve rotor slip problems, in this study [19].

II. THE MODELLING OF THE HYTERESIS MOTOR

Some parameters are considered constant as permeability of hysteresis material for hysteresis motor modelling with sinusoidal distributed and balanced winding. The permanent magnet structure can be modelled as a constant current source I_m . The resistor R_e expresses the Eddy current effect. Hysteresis effect is expressed with the hysteresis resistance R_h and the equivalent hysteresis inductance L_h . These two parameters hysteresis are a function of parallel path angle, δ . Hysteresis ring consists of two parts as inner ring and outer ring. The resistances and inductances of these parts can be

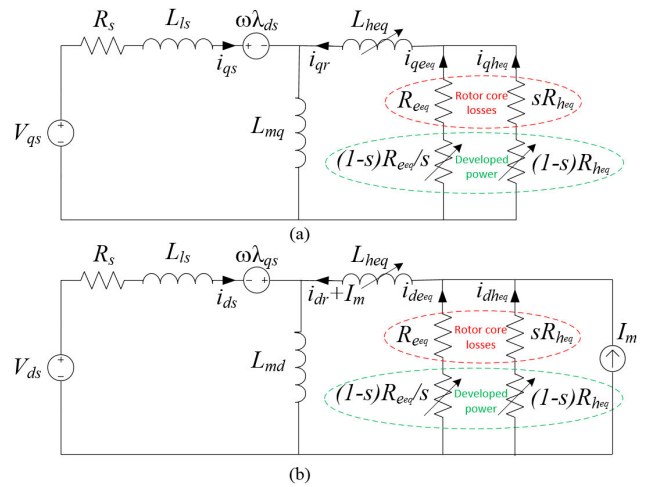


FIGURE 2. Electrical equivalent circuits: (a) q-axis and (b) d-axis.

represented by the expressions given in (1) - (4). The magnetic inductance can be determined as given in (5). The resistances and inductances in equivalent circuits are used in the dq -model. The equivalent circuit resistances and inductances can be determined as $R_{eeq} - R_{heq}$ and $L_{eeq} - L_{heq}$, respectively.

$$R_{h(inner)} = \frac{3K_w^2 N_w^2 V_{h(inner)} \mu}{\mu^2 r_r(inner)} \sin \delta \quad (1)$$

$$R_{h(outer)} = \frac{3K_w^2 N_w^2 V_{h(outer)} \mu}{\mu^2 r_r(outer)} \sin \delta \quad (2)$$

$$L_{h(inner)} = \frac{3K_w^2 N_w^2 V_{h(inner)} \mu}{\mu^2 r_r(inner)} \cos \delta \quad (3)$$

$$L_{h(outer)} = \frac{3K_w^2 N_w^2 V_{h(outer)} \mu}{\mu^2 r_r(outer)} \cos \delta \quad (4)$$

$$L_m = \frac{6K_w^2 N_w^2 V_{h(inner)} \mu_0 r_g l}{\pi p^2 l_g} \quad (5)$$

where ω is the angular frequency, V_h is the volume of the hysteresis ring, r_r is the radius of hysteresis ring, r_g is the mean radius of the air-gap, l_g is the radial length of the air-gap. L_{mq} and L_{md} are assumed as equal to L_m because there is not any saliency on the rotor structure. The model has two components as hysteresis and eddy. These components are the losses occurring in the rotor. The hysteresis loss is indicated as sR_h and the eddy current loss is expressed as R_e . The other resistor represents the motor output power. s is slip of the rotor, $((1-s)/s)R_e$ is the effective eddy current and $(1-s)R_h$ is hysteresis resistance. The rotor losses occur when the rotor speed is different from the synchronous speed. If the rotor is reached up to the synchronous speed, these losses will also be reduced. The motor torque is generated with permanent magnet and hysteresis ring during the start. The shaft torque continues to be produced by means of permanent magnets after synchronization is achieved [20].

dq -axis motor electrical equivalent circuits are given in Figure 2. The dq -axis equations of the motor can be

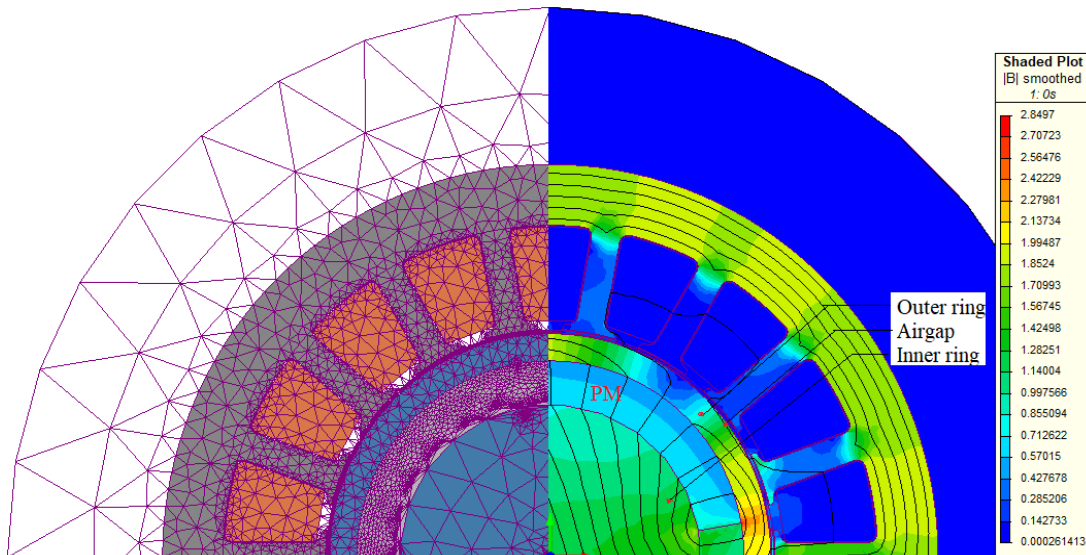


FIGURE 3. Motor mesh view and flux lines for FEA.

derived from the equivalent circuit and it can be expressed by equations given as follows [21]. The dq -model voltages of stator and rotor are given from (6) to (9). Also, the motor's flux linkage can be specified by (10) to (13). The generated electrical torque is given in (14).

$$V_{qs} = R_s I_{qs} + \frac{d\lambda_{qs}}{dt} + \omega_r \lambda_{ds} \quad (6)$$

$$V_{ds} = R_s I_{ds} + \frac{d\lambda_{ds}}{dt} - \omega_r \lambda_{qs} \quad (7)$$

$$V_{qr} = R_r I_{qr} + \frac{d\lambda_{qr}}{dt} = 0 \quad (8)$$

$$V_{dr} = R_r I_{dr} + \frac{d\lambda_{dr}}{dt} = 0 \quad (9)$$

$$\lambda_{qs} = I_{qs} (L_{mq} + L_{ls}) + L_{mq} (I_{qe_{eq}} + I_{qh_{eq}}) \quad (10)$$

$$\lambda_{ds} = I_{ds} (L_{md} + L_{ls}) + L_{md} (I_{de_{eq}} + I_{dh_{eq}} + I_m) \quad (11)$$

$$\lambda_{qr} = (I_{qe_{eq}} + I_{qh_{eq}}) (L_{heq} + L_{mq}) + L_{mq} I_{qs} \quad (12)$$

$$\lambda_{dr} = (I_{de_{eq}} + I_{dh_{eq}}) (L_{heq} + L_{md}) + L_{md} (I_{ds} + I_m) \quad (13)$$

$$T_e = \frac{3}{2} (\lambda_{ds} I_{qs} - \lambda_{qs} I_{ds}) \quad (14)$$

where R_s is the stator phase resistance, L_{ls} is the leakage inductance per stator phase, L_{mq} and L_{md} are the dq -axis magnetizing inductance, and ω_r is the angular frequency of the rotor, V_{qs} and V_{ds} are the dq -axis stator induction voltages, V_{qr} and V_{dr} are the dq -axis rotor induction voltages, λ_{qs} and λ_{ds} is the qd -axis stator flux coupling, T_e is the developed electrical torque.

III. DESIGN OF THE PMHSM

The proposed motor is designed by using the Motor-Solve program. The motor is also analyzed with FEA via Magnet program. The detailed structure of the stator and rotor is given in Figure 3. The stack length of stator is 70 mm and the copper windings are used as a single layer.

The inner-hysteresis ring of the rotor is taken as $\Delta di=8.7$ mm and the outer-hysteresis ring of the rotor is taken as $\Delta do=2$ mm. The rings are made from the same material. The thickness of the outer ring is very important to produce the required torque during the starting of the motor. The permanent magnets are placed between the two rings. The thickness of the magnets is 4mm. The material of the magnets is taken as Neodymium Iron Boron (NdFeB-30/27) alloy to obtain high magnetic field. The air-gap between the stator and the rotor is 0.3 5mm, stator lamination material is M470-50A and skew angle is determined as 6° to obtain more low torque ripples. The stator slot number is taken as 24 and the coil pitch is 12. The fill rate of the stator is determined as 40%. The hysteresis rings of the rotor are made of silicon steel. This material has some superior properties such as low iron losses, high magnetic induction and high operating frequencies. The permanent magnets placed between the hysteresis rings. The flow of the magnetic flux lines in the outer hysteresis ring, magnets and inner ring can be seen in detail in Figure 4. If Figure 3 and Figure 4 examined together, it is understood that the magnetic flux orientation creates a closed-loop motion between the stator and the rotor. The resulting flux distribution has a deviation in the outer ring and air gap. The flux lines have a deviated angle when passing from the stator teeth to outer ring. In the next stage, the flux lines continue to the core that they should keep their direction again in the flux loop. This deviation shows that the rotor is locked to the stator rotating field. Thus, the synchronization procedure has been achieved in this study. If this deviation cannot be created in the outer ring, the motor will not start without any auxiliary devices. On the other hand, it follows the path of radial direction in the magnets. It can be said that the outer hysteresis ring thickness plays an important role in the magnetic flux orientation especially during start-up. The optimum thickness of outer ring was determined to be

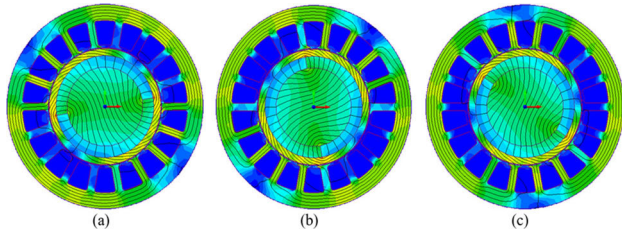


FIGURE 4. Flux function contour at- (a) 0ms, (b) 5ms, (c) 7.5ms.

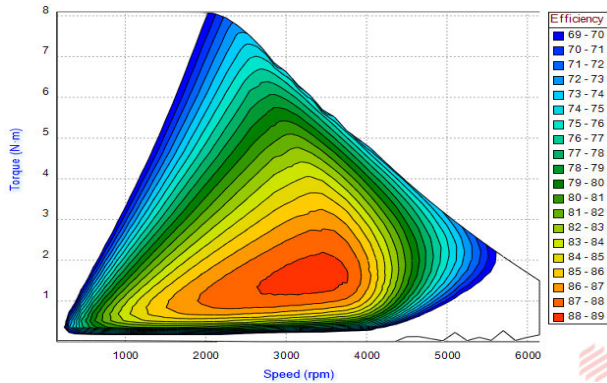


FIGURE 5. Efficiency map.

2 mm with various simulations for the designed motor. Since the thickness of the rotor shaft was not interfered, the inner ring thickness naturally appeared. The maximum value of the flux density is 2.44 T, which is occurred in the pole junction region of the permanent magnets. The inner hysteresis ring is used in order to provide a path to the magnetic flux loop. are not interfered. The shaft has the required mechanical strength; it also creates a flux loop path for the magnetic flux.

The flux function contour at 0 ms, 5 ms, 7.5 ms are illustrated in Figure 4. in order to show the rotating operation by rotating magnetic field produced by three-phase grid.

The efficiency map of the designed motor is given in Fig. 5. The efficiency of the motor is changed from 70% to 89% for rated speed (3000 rpm). However, a conventional induction motor as same power to the designed motor has 72% efficiency.

The moment of the inertia is 0.00026875 kg.m². The ratio of inertia moment to load torque is calculated as 405.605 μm. Mass of motor is 2.92 kg. The ratio of the power to volume is calculated as 4.9 kW/m³ without considering the motor case.

A pump load was used in this study. So that, the load does not require a higher starting torque from the motor during the starting stage. The designed motor cannot be used any loads such as; conveyor, punch press, mixer, crane, etc. Because, the proposed motor has low starting torque. The motor dynamics is appropriated for low starting torque such as fans and pumps loads. If a higher starting torque is needed in an application, the voltage of the stator winding should be increased in order to obtain a high inrush current. A delta-wye starting procedure can be used in order to obtain higher starting torque.

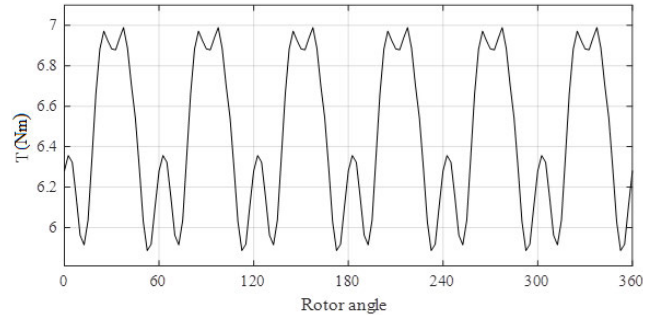


FIGURE 6. shaft torque of the designed motor operating at the steady-state.

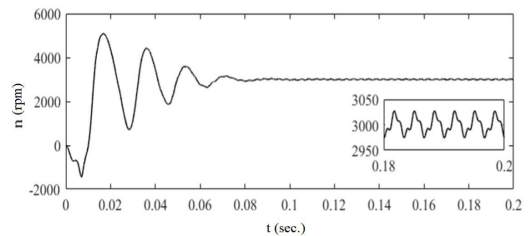
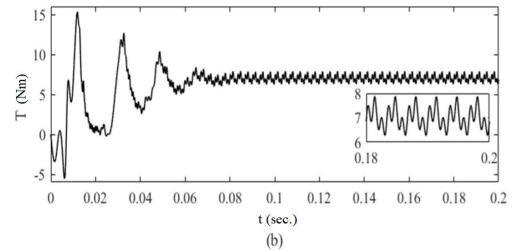
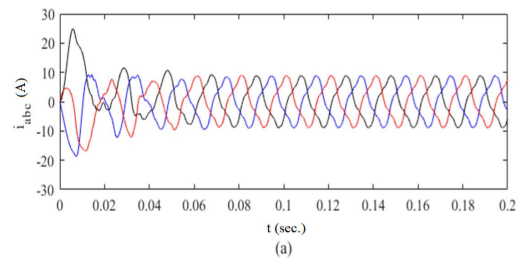


FIGURE 7. Self-starting performance of PMHSM. (a) Stator currents, (b) Torque, (c) Speed.

IV. PERFORMANCE ANALYSIS OF THE PMHSM

The torque of the motor in the steady-state is given in Figure 6. by using FEA. The result was obtained by using a constant current source. It can be said that the shaft torque ripple for the submersible pump motor is acceptable level.

The load tests of the designed motor were performed by using MATLAB Magnet-Simulink plugin. The motor is directly connected to the network in order to analyze self-starting feature as shown in Figure 7.

A photo is given as illustrated in Figure 8. to show the dimensional differences between a traditional induction motor based submersible pump motor and the designed motor. The stack length of the designed motor is about half length of the traditional pump motor. The stack lengths of the stator/rotor core are taken as 70 mm for the designed motor.

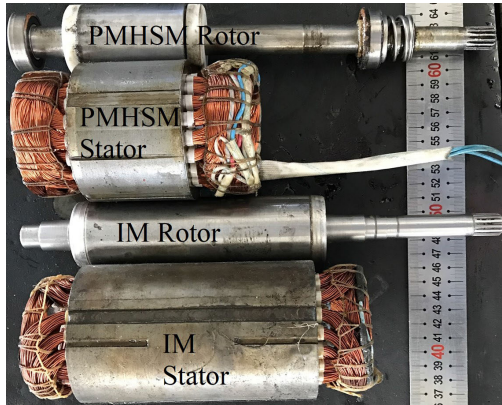


FIGURE 8. The stator/rotor structures of the designed PMHSM and the IM.

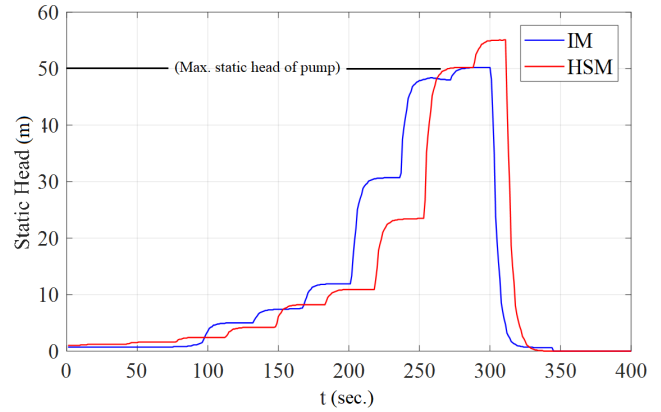


FIGURE 10. The pumping height performance of the PMHSM and IM.

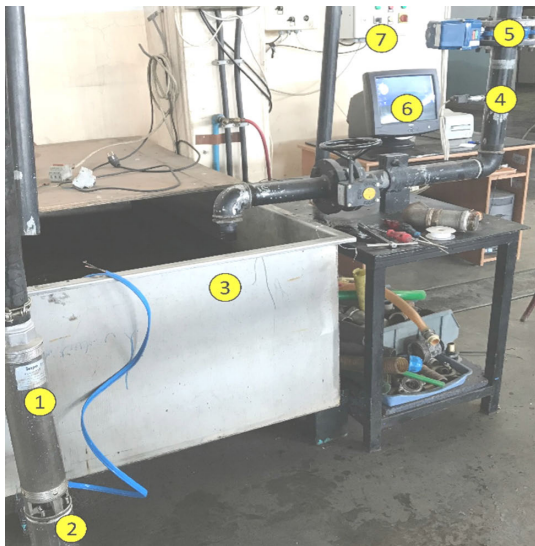


FIGURE 9. The experimental setup.

However, the stator/rotor lengths are about 170 mm for the traditional motor with the power 2 HP. The designed motor and the traditional IM motor were connected to the same pump to compare the water static head.

The designed prototype motor and a commercial submersible pump motor have been tested by using same experimental setup as illustrated in Figure 9. In this figure, the experimental setup and its components are given in the figure with labelled explanations as follows;

- (1) Submersible pump,
- (2) Electric motor,
- (2) Water tank,
- (4) Pressure transmitter,
- (5) Electromechanical valve,
- (6) Measuring computer,
- (7) Electric panel.

The static head is an important parameter for pumping systems. The static head is the pressure resulting from a column of liquid acting under gravity. It may be called pumping height as simple. The test results for determining the performance of both pump systems is given in Figure 10.

TABLE 1. Comparisons of traditional IM and PMHSM.

Motor	IM	PMHSM
Speed (rpm)	2810	3000
Current (A)	4.4	5.1
Cos ϕ	0.73	0.86
Efficiency (%)	72	79
Static Head (m)	50	55
Total Cost (\$)	175	160
Torque	7.1	4.78
Torque Ripple (%)	20	16

A commercial submersible pump with a rated static head 50 m was used (Brand: IMPO, Type: SK406/09). The induction motor was able to reach up maximum static head as 50.2 m. The designed prototype motor was able to reach up 55.1 m maximum static head at the same test conditions as shown in Figure 10.

V. CONCLUSION

Commercial pump motors are usually driverless since they can be designed for economic reasons. Therefore, conventional IM motors are generally preferred. This study is proposing a motor which is driverless and more efficient than IM motors. This performance effect can be seen in Table 1. In this study, PMHSM is designed with a new rotor structure for use in pump applications. A commercial three-phase submersible pump motor is modified for verification tests. A standard pump was used during the tests in this work. The stator stack length is reduced as half of the standard length and stator winding is rearranged for the new design. The rotor is formed by buried magnets between the two rings. The designed motor is developed in order to connect to an existing three-phase grid that does not require a driver. The motor performance tests are performed in Sezgin Motor Company. It has been showed that the starting feature of the motor is suitable for pump applications. However, sufficient torque could not be produced for high starting torque requirements. The motor starting current can be increased in order to

overcome this problem. In the same test equipment are used to obtain a good comparison between commercial IM and designed PMHSM. The IM is connected to the same pump and same test procedure. The same performance tests were performed for IM. It has been seen that the performance of PMHSM is better than the IM. The following advantages are achieved;

- Low vibration noise,
- High power/volume,
- Increasing static head,
- Simplest manufacturing of rotor structure,
- No contains copper loss in rotor,

Designed motor-driven pump applications are particularly important for producing high shaft speeds that are essential for submersible-pump systems, fire pump systems, oil well pump units and jet pumps. Because the static head can be increased by the square of the motor shaft speed in such applications. Future works is listed as below;

- The geometry optimization of the rotor,
- Research on ring materials,
- Current harmonic eliminations,
- Improve the start-up capability for overload,
- Single phase motor study for home applications.

APPENDIX

The phase to phase supply voltage is 380V, the source frequency is 50Hz, the output power is 2.2kW, torque constant K_t is 1.24 Nm/A, L_d is 40.8 mH, L_q is 76.6 mH, R_s is 6.67 Ω .

REFERENCES

- [1] B. K. Bose, "Global warming: Energy, environmental pollution, and the impact of power electronics," *IEEE Ind. Electron. Mag.*, vol. 4, no. 1, pp. 6–17, Mar. 2010.
- [2] G. Boztas, O. Aydogmus, M. Caner, and H. Guldemir, "Design, optimisation and implementation of low-voltage synchronous reluctance motor for solar-powered systems," *IET Power Electron.*, vol. 12, no. 7, pp. 1679–1685, Jun. 2019.
- [3] P. A. M. Dirac, "The lorentz transformation and absolute time," *Physica*, vol. 19, nos. 1–12, pp. 888–896, 1953, doi: 10.1016/S0031-8914(53)80099-6.
- [4] C. Verucchia, C. Ruschetti, E. Giraldo, G. Bossiob, and J. Bossiob, "Efficiency optimization in small induction motors using magnetic slot wedges," *Electr. Power Syst. Res.*, vol. 152, pp. 1–8, Nov. 2017.
- [5] O. Misir, S. Raziee, N. Hammouche, C. Klaus, R. Kluge, and B. Ponick, "Prediction of losses and efficiency for three-phase induction machines equipped with combined star-delta windings," *IEEE Trans. Ind. Appl.*, vol. 53, no. 4, pp. 3579–3587, Jul./Aug. 2017.
- [6] X. Chen and C. Gu, "Research on operating performance for hybrid rotor synchronous motor," *Elektron Ir Elektrotehnika*, vol. 3, pp. 3–8, Sep. 2011.
- [7] D. Cardwell and D. Ginle, *Handbook of Superconducting Materials*. Boca Raton, FL, USA: CRC Press, 2003.
- [8] J. Nitao, E. Scharlemann, and B. Kirkendall, "Equivalent circuit modeling of hysteresis motors," LLNL, Livermore, CA, USA, Tech. Rep. TR-416493, 2009.
- [9] M. Jagiela, T. Garbiec, and M. Kowol, "Design of high-speed hybrid hysteresis motor rotor using finite element model and decision process," *EEE Trans. Magn.*, vol. 50, no. 2, Feb. 2014, Art. no. 7021304, doi: 10.1109/TMAG.2013.2284018.
- [10] R. Qin and M. A. Rahman, "Magnetic equivalent circuit of PM hysteresis synchronous motor," *IEEE Trans. Magn.*, vol. 39, no. 5, pp. 2998–3000, Sep. 2003.
- [11] A. Darabi, S. Mohsen, and T. Ghanbari, "Coreless dual-rotor disc hysteresis motor, modeling, and performance prediction," *Electr. Power Compon. Syst.*, vol. 38, no. 5, pp. 575–591, 2010, doi: 10.1080/15325000903376909.
- [12] R. T. Ugale, B. N. Chaudhari, S. Baka, and A. Pramanik, "A hybrid interior rotor high-performance line start permanent magnet synchronous motor," *Electr. Power Compon. Syst.*, vol. 42, no. 9, pp. 901–913, 2014.
- [13] M. Azari and M. Mirsalim, "Performance analysis of a line start permanent magnet motor with slots on solid rotor using finite element method," *Electr. Power Compon. Syst.*, vol. 41, no. 12, pp. 1159–1172, 2013, doi: 10.1080/15325008.2013.809819.
- [14] S. Boroujeni, M. Haghparast, and N. Bianchi, "Optimization of flux barriers of line-start synchronous reluctance motors for transient- and steady-state operation," *Electr. Power Compon. Syst.*, vol. 43, no. 5, pp. 594–606, 2015, doi: 10.1080/15325008.2014.984819.
- [15] M. A. Rahman and R. Qin, "A permanent magnet hysteresis hybrid synchronous motor for electric vehicles," *IEEE Trans. Ind. Electron.*, vol. 44, no. 1, pp. 46–53, Feb. 1997.
- [16] J. Qian and M. A. Rahman, "Analysis of field oriented control for permanent magnet hysteresis synchronous motors," *IEEE Trans. Ind. Appl.*, vol. 29, no. 6, pp. 1156–1163, Nov./Dec. 1993.
- [17] M. A. Rahman, M. A. Copeland, and G. R. Slemmon, "An analysis of the hysteresis motor PART III: Parasitic losses," *IEEE Trans. Power Appl.*, vol. PAS-88, no. 6, pp. 954–961, Jun. 1969.
- [18] K. Kurihara and M. A. Rahman, "Transient performance analysis for permanent-magnet hysteresis synchronous motor," *IEEE Trans. Ind. Appl.*, vol. 40, no. 1, pp. 135–142, Jan./Feb. 2004.
- [19] M. Gedikpinar and O. Aydoğmuş, "Design of a self-starting hybrid permanent magnet hysteresis synchronous motor connected directly to the grid," *Turkish J. Elect. Eng. Comput. Sci.*, vol. 25, no. 3, pp. 1657–1668, 2017.
- [20] S. F. Rabbi and M. A. Rahman, "Equivalent circuit modeling of an interior permanent magnet hysteresis motor," in *Proc. IEEE 27th Can. Conf. Elect. Comput. Eng. (CCECE)*, May 2014, pp. 1–5.
- [21] M. A. Rahman and R. Qin, "Starting and synchronization of permanent magnet hysteresis motors," *IEEE Trans. Ind. Appl.*, vol. 32, no. 5, pp. 1183–1189, Sep. 1996.



MEHMET GEDİKPINAR received the B.S. degree from the Department of Electrical Education, Gazi University, Ankara, Turkey, in 1981, the M.Sc. degree from the Institute of Science and Technology, Firat University, in 1998, and the Ph.D. degree from THE Institute of Science and Technology, Gazi University, in 2002. He is currently working as an Associate Professor with the Department of Electrical and Electronics, Faculty of Technology, Firat University. His research interests include intelligent control, electrical machines and designing, electronics instruments and measurements, and analyzing of circuit.

•••